Organic & Biomolecular Chemistry

ROYAL SOCIETY OF CHEMISTRY

PAPER

View Article Online
View Journal | View Issue

Cite this: *Org. Biomol. Chem.*, 2021, **19**, 4986

Tuning the exchange dynamics of boronic acid hydrazones and oximes with pH and redox control†

Gun Su Han and Dylan W. Domaille *

Dynamic bonds continually form and dissociate at equilibrium. Carbonyl compounds with proximal boronic acids, including 2-formylphenylboronic acid (2-FPBA), have been reported to form highly dynamic covalent hydrazone and oxime bonds in physiological conditions, but strategies to tune the dynamics have not yet been reported. Here, we characterize the dynamics of 2-FPBA-derived hydrazones and oximes and account for both the rapid rate of formation (~10^2–10^3 M^{-1} s^{-1}) and the relatively fast rate of hydrolysis (~10^{-4} s^{-1}) at physiological pH. We further show that these substrates undergo exchange with α-nucleophiles, which can be reversibly paused and restarted with pH control. Finally, we show that oxidation of the arylboronic acid effectively abolishes the rapid dynamics, which slows the forward reaction by more than 30 000 times and increases the hydrolytic half-life from 50 minutes to 6 months at physiological pH. These results set the stage to explore these linkages in dynamic combinatorial libraries, reversible bioconjugation, and self-healing materials.

Received 1st February 2021,
Accepted 12th May 2021

DOI: 10.1039/d1ob00191d

rsc.li/obc

Introduction

Dynamic covalent bonds (DCBs) are reversible covalent bonds at thermodynamic equilibrium.[1–3] Two of the most commonly used DCBs are hydrazones and oximes, formed from an aldehyde or ketone and a hydrazine or alkoxyamine, respectively.[4–11] As a result of their broad availability, ease of incorporation into more complex (macro)molecules, and ability to exchange, hydrazones and oximes have been used to reversibly tag biomolecules[12] and select for self-assembled inhibitors in protein-directed dynamic combinatorial chemistry.[13]

One of their biggest limitations in dynamic processes, however, is the relatively slow rates of formation and exchange in aqueous solvents.[13] Aniline-based organocatalysts accelerate the kinetics, but the need for a high catalyst concentration (>50 mM) limits the broad use of this strategy, especially for live-cell labeling applications.[14,15] Neighboring group activation provides a complementary approach[16–19] to increase the rate of hydrazones and/or oximes formation.[20–22] A variety of functional groups proximal to the reacting carbonyl, including *o*-pyridyl,[16] *o*-phosphate,[17] *o*-formyl,[18] and *o*-boronic acids dramatically accelerate the rate of formation of hydrazones and/or oximes.[20–22] Of these, *o*-boronic acids are especially active neighboring groups, accelerating hydrazone and oxime formations several orders of magnitude faster than hydrazone/oxime formations with benzaldehyde.

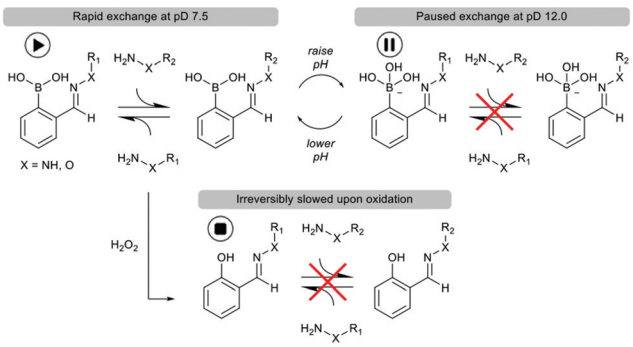

Fig. 1 2-FPBA-derived hydrazones and oximes are activated by the proximal boronic acid and Brønsted acid catalysis. We hypothesized that the dynamics could be reversibly paused and activated with pH control and irreversibly slowed by oxidizing the boronic acid with H_2O_2.

Though the reaction between and α-nucleophiles and *o*-boronic aryl aldehydes/ketones dates back more than sixty years,[23–26] only recently have these reactions been shown to proceed exceptionally fast in physiological conditions, even at micromolar concentrations.[20,21,27,28] Despite their emerging importance in site-specific bioorthogonal labels,[29,30] oxida-

Department of Chemistry, Colorado School of Mines, Golden, CO, USA.
E-mail: ddomaille@mines.edu

†Electronic supplementary information (ESI) available. See DOI: 10.1039/d1ob00191d

tively activated metal chelators,[31–33] and potential for use in dynamic combinatorial libraries, a comprehensive characterization of the reversible dynamics of hydrazones and oximes with neighboring boronic acids, susceptibility to exchange, and responsivity to common molecular inputs has not been reported.

Here, we characterize highly dynamic 2-formylphenylboronic acid (2-FPBA)-derived hydrazone and oxime bonds by accounting for both the rapid rate of formation (~10^2–10^3 M^{-1} s^{-1}) and the relatively fast rate of hydrolysis ($t_{1/2}$ ~50 minutes) at physiological pH. We demonstrate that the resulting hydrazone/diazaborine or oxime can exchange with another α-nucleophile and that the exchange can be temporarily paused and restarted with pH control. Finally, we highlight that treatment with H_2O_2 oxidizes the arylboronic acid catalyst to a far less active hydroxyl group, effectively abolishing the rapid dynamics (Fig. 1). Taken together, our studies demonstrate that the rapid dynamics of 2-FPBA-derived hydrazones and oximes can be reversibly sped up and slowed down and irreversibly abolished with simple molecular inputs. These results provide a powerful way to tune the exchange dynamics of this class of dynamic bonds, setting the stage to explore their utility in reversible bioconjugation reactions and dynamic combinatorial library generation.

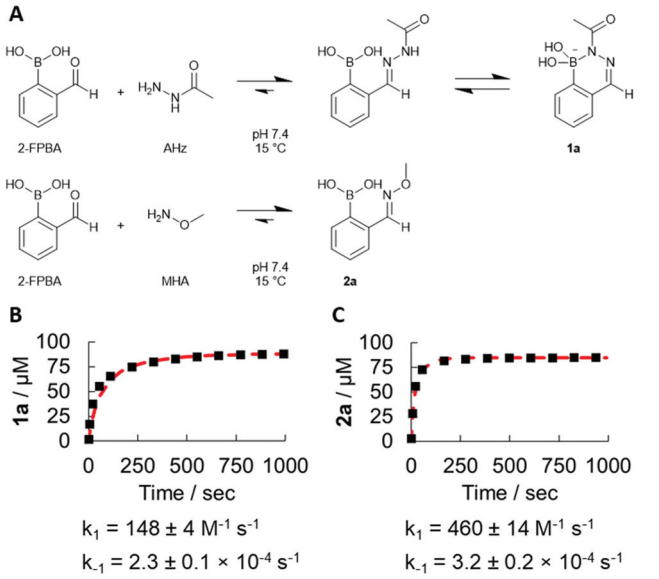

Fig. 2 2-FPBA forms highly dynamic hydrazone and oxime bonds. (A) The reaction kinetics were measured for 2-FPBA and AHz and for 2-FPBA and MHA. (B) Formation of **1a** was monitored as a function of time. (C) Formation of **2a** was monitored as a function of time. The red line represents a fit to the kinetic model. Kinetic traces were repeated in triplicate; rate constants are reported as the average of three runs with independent fitting to the model ± SD.

Results and discussion

2-Formylphenylboronic acid (2-FPBA) has previously been shown to form a hydrazone or oxime at an exceptionally fast rate. The rate acceleration has been attributed to the intramolecular catalytic effect of *o*-boronic acid.[20] To confirm the proximity effect of the boronic acid, we measured the rate of hydrazone and oxime formations from 2-FPBA and its *para*-isomer, 4-formylphenylboronic acid (4-FPBA) with acethydrazide (AHz) and *O*-methylhydroxylamine (MHA) as model hydrazide and alkoxyamine nucleophiles, respectively. 4-FPBA was combined with equimolar AHz or MHA (1.85 mM) in phosphate buffer (PB, 200 mM, pD 7.5) at room temperature, and product formation was monitored with time-course NMR spectroscopy. The reaction between 4-FPBA and MHA proceeds with a rate constant of 3.3 × 10^{-2} M^{-1} s^{-1}, while the reaction between 4-FPBA and AHz is roughly 10-fold slower (k_1 = 3.8 × 10^{-3} M^{-1} s^{-1}) (Fig. S1†).

When we repeated the experiment with the *ortho*-isomer 2-FPBA, the product formation was too fast to monitor with NMR spectroscopy. Instead, time-course ultraviolet-visible spectroscopy (UV-vis) was used to track product formation. 2-FPBA (100 μM) was combined with equimolar AHz or MHA (100 μM) in phosphate buffer (PB, 100 mM, pD 7.5) at 15 °C, and product formation was monitored with UV-visible spectroscopy. As reported by the Bane group, the reaction of 2-FPBA and AHz initially forms a hydrazone, which, in aqueous solution, rapidly equilibrates with its cyclized product, diazaborine (DAB) (Fig. 2A, **1a**).[21,27] The reaction of 2-FPBA and MHA yields oxime **2a** (Fig. 2A, **2a**). An irreversible second-order model fits the data poorly (Fig. S2†). We hypothesized that proximal boronic acid was also accelerating the rate of hydrolysis and fitted the data to a reversible model that is second-order in the forward direction (k_1) and first-order in hydrolysis in the back reaction (k_{-1}).[4] This provides an excellent fit to the kinetic data.

The reaction between 2-FPBA and AHz proceeds rapidly (k_1 = 148 ± 4 M^{-1} s^{-1}) with concomitant rates of hydrolysis six orders of magnitude slower (k_{-1} = 2.3 ± 0.1 × 10^{-4} s^{-1}; $t_{1/2}$ ~50 minutes) at 15 °C (Fig. 2B). At pD 7.5, we observed only DAB **1a** (Fig. S3†). The reaction between 2-FPBA and MHA forms **2a** quickly and hydrolyzes at a relatively fast rate (k_1 = 460 ± 14 M^{-1} s^{-1} and k_{-1} = 3.2 ± 0.2 × 10^{-4} s^{-1}, respectively) (Fig. 2C). The dramatic rate difference between hydrazone or oxime formation from 2-FPBA compared to 4-FPBA supports the idea that the rapid rate acceleration originates from a neighboring group effect of the boronic acid. It is also important to note that the presence of the *o*-boronic acid accelerates the hydrolysis of the diazaborine and oxime, and the back rate of hydrolysis must be accounted for when measuring the kinetics of this class of compounds.

Next, we completed the same kinetic analysis at 35 °C, 55 °C, and 75 °C for the formations of **1a** and **2a**. Eyring analysis yielded activation parameters of $\Delta H^{\ddagger}$ = 13.3 kJ mol^{-1} and $\Delta S^{\ddagger}$ = −157 J mol^{-1} to form **1a** and $\Delta H^{\ddagger}$ = 59.0 kJ mol^{-1} and $\Delta S^{\ddagger}$ = −109 J mol^{-1} to re-form 2-FPBA and AHz (Fig. S4A and B†). At room temperature, this corresponds to a low energy barrier to formation ($\Delta G^{\ddagger}$ = 60 kJ mol^{-1}) with a higher energy barrier to hydrolysis ($\Delta G^{\ddagger}$ = 91 kJ mol^{-1}). Oxime **2a** has activation parameters of $\Delta H^{\ddagger}$ = 18.6 kJ mol^{-1} and $\Delta S^{\ddagger}$ = −129 J K^{-1}

mol^{-1} to form **2a** and $\Delta H^{\ddagger}$ = 57.4 kJ mol^{-1} and $\Delta S^{\ddagger}$ = −111 J K^{-1} mol^{-1} to re-form the constituent 2-FPBA and MHA building blocks. At room temperature, oxime formation proceeds with a low energy barrier of $\Delta G^{\ddagger}$ = 57 kJ mol^{-1} and a higher barrier of $\Delta G^{\ddagger}$ = 91 kJ mol^{-1} to hydrolysis (Fig. S4C and D†).

Hydrazone and oxime formations are well-established to be dependent on pH conditions.[27,34] To explore how sensitive the dynamics of this particular class of 2-FPBA-derived hydrazones/diazaborines and oximes are to pH, we measured the kinetics of formation and hydrolysis of **1a** and **2a** at 15 °C at pH 6.5, 7.4, 8.5, 9.5, and 12.0. Because our kinetic analysis enables the extraction of both k_1 and k_{-1}, we can delineate the influence of pH on each process independently. Within the explored range of pH, k_1 and k_{-1} decrease as a function of pH, resulting in three orders of magnitude difference in the rates between pH 6.5 and 12.0 (Fig. 3A and B). The K_{eq} for DAB **1a** reaches a maximum at pH 8.5, and then decreases slightly at higher pH conditions (Fig. 3C). We attribute the lowest K_{eq} at pH 6.5 to increased formation of acyl hydrazone, which is hydrolytically less stable than DAB **1a**. The mechanistic origin of why the K_{eq} of DAB **1a** reaches a maximum at pH 8.5 is not immediately apparent. The K_{eq} for oxime **2a** trends downward as the pH increases (Fig. 3D). From pH 6.5–12, DAB **1a** and oxime **2a** show K_{eq} values on the order of 10^5–10^6 despite large changes in their k_1 and k_{-1} values.

Accessing facile exchange chemistry is a central component to identifying reactions for dynamic combinatorial chemistry and reversible bioconjugation. Because k_1 and k_{-1} are sensitive to pH, we reasoned that the rate of hydrazone exchange of **1a** or oxime exchange of **2a** could be controlled by simply altering the pH of the solution. To explore this idea, we investigated how **1a** exchanges with a competing hydrazide. **1a** was formed *in situ* in pD 7.5 in buffered D_2O (200 mM PB). We surveyed a range of competing hydrazides, including bulky hydrazides (pivalic acid hydrazide (PivHz), isobutyric acid hydrazide (iBHz), and *tert*-butylcarbazate (tBCz)), as well as an electron-deficient hydrazide (cyanoacetohydrazide (CAHz)).

The hydrazides show different extents of exchanges that are dependent on their steric effects (Fig. 4A). While PivHz shows no exchange with DAB **1a** (Fig. 4A, (x); Fig S5a and b†) and iBHz shows limited exchange (Fig. 4A (◆); Fig. S6a and b†), tBCz, which has its *tert*-butyl group one atom farther from the hydrazide compared to pivalic acid hydrazide, exchanges and equilibrates to 92% **1e** after 10 hours (Fig. 4A (□); Fig. S7a and b†). CAHz also exchanges with **1a** and equilibrates to 84% **1d**, despite the inclusion of a strong electron-withdrawing group (Fig. 4A (▲); Fig S8a and b†). Repeating the same experiments at pD 12.0 led to no measurable exchange after 15 hours for all hydrazides (Fig. S9–S12†).

We next investigated how oxime **2a** exchanges with a range of increasingly bulky alkoxyamines, including *O*-ethylhydroxylamine (EHA), *O*-isopropylhydroxylamine (iPHA), and *O*-*tert*-butylhydroxylamine (t-BHA). All alkoxyamines, including the very bulky t-BHA, exchange (Fig. 4B; ESI Fig. S13a–S15b†). There is a slight increase in exchange as the size of the alkyl group increases; however, steric effects do not affect the exchange to the same degree as they do in the hydrazide examples. We attribute the difference in the exchange behaviors between the diazaborines and oximes to the absence of the hetereocyclic ring in case of the oximes. Similar to the results we observed with hydrazone exchange, oxime exchanges were significantly slower at pD 12.0. Less than 10% exchange was observed after 14 hours for each alkoxyamine (Fig. S16–S18†).

Next, we turned to using pD as an easily reversible switch to pause and restart the exchange process. When **1a** was formed *in situ* from AHz (3 equiv.) at pD 7.5 and treated with tBCz (0.5

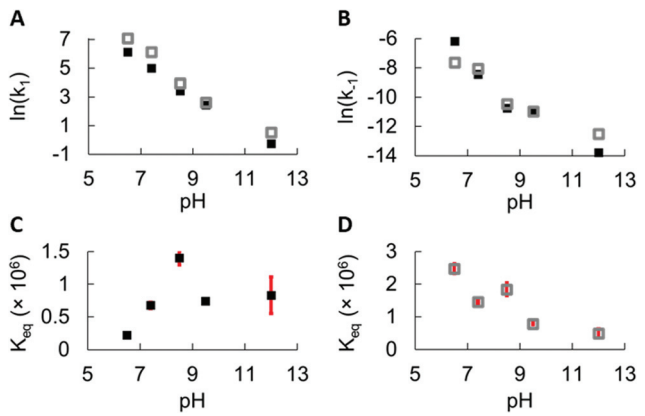

Fig. 3 Effect of pH on the rate of formation and hydrolysis of **1a** and **2a**. (A) k_1 rates of **1a** (filled squares) and oxime **2a** (empty squares) as a function of pH. (B) k_{-1} rates of **1a** (filled squares) and **2a** (open squares). (C) K_{eq} values **1a** as a function of pH. (D) K_{eq} values for oxime **2a**. Values were measured in triplicate. Error bars represent S.D. of three independent measurements.

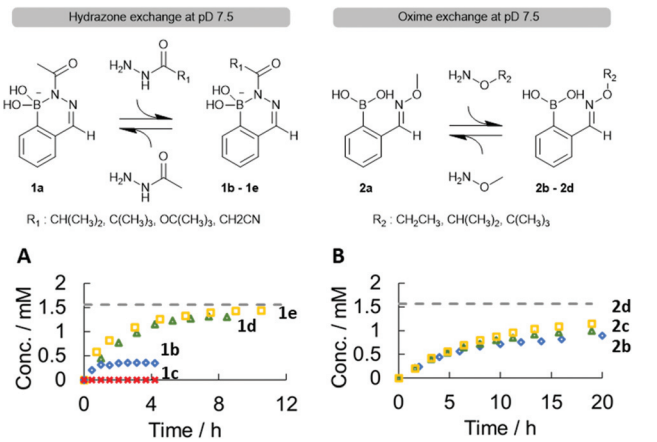

Fig. 4 Exchange of **1a** with a range of acylhydrazides and exchange of **2a** with a range of alkoxyamines. (A) **1a** was formed *in situ* from 2-FPBA and AHz (3 equiv.) in aqueous buffer (200 mM PB, pD 7.5) and subsequently treated with either iBHz (3 equiv.) to give **1b** (◆), PivHz (3 equiv.) to give **1c** (x), CAHz (3 equiv.) to give **1d** (▲), or tBCZ (3 equiv.) to give **1e** (□). (B) **2a** was formed *in situ* from 2-FPBA and MHA (3 equiv.) in aqueous buffer (200 mM PB, pD 7.5) and subsequently treated with either EHA (3equiv.) to form **2b** (◆), iPHA (3 equiv.) to form **2c** (▲), and t-BHA (3 equiv.) to form **2d** (□).

equiv.), the ratio of **1a**:**1e** equilibrates to 57:43 (Fig. 5A). However, when the pD was adjusted to 12.0 before adding tBCz (0.5 equiv.), no exchange was observed for 15 hours (Fig. 5B). The difference in the exchange behaviors inspired us to explore subsequent exchanges with pD control. **1a** was formed *in situ* from AHz (3 equiv.) and treated with tBCz (0.5 equiv.) at pD 7.5 in buffered D_2O. After the initial exchange was complete, 2.5 equivalents of tBCz were added, and the exchange was monitored with time-course NMR spectroscopy (Fig. 5C). The subsequent exchange finished in 6 hours with 88% **1e**. However, when we adjusted the pD to 12 prior the addition of 2.5 equivalents of tBCz, no subsequent exchange was observed. When the pD was readjusted to 7.5, the exchange immediately resumed; after 7 hours, the mixture equilibrated to 88% **1e** again (Fig. 5D).

In the case of oxime exchange, methyloxime **2a** and ethyloxime **2b** are of similar thermodynamic stability (Fig. 6A) and undergo pH-dependent exchange, which significantly slows down at pD 12.0 (Fig. 6B). We thus reasoned that the amount of **2a** or **2b** can be controlled with off-stoichiometric control of the nucleophile. Oxime **2a** was formed *in situ* from MHA (3 equiv.) and treated with EHA (3 equiv.) at pD 7.5 in buffered D_2O. After the initial exchange was complete with ~50% of each oxime, 24 equivalents of MHA were added, and the exchange was monitored with time-course NMR spectroscopy (Fig. 6C). The subsequent exchange finished in 20 hours with

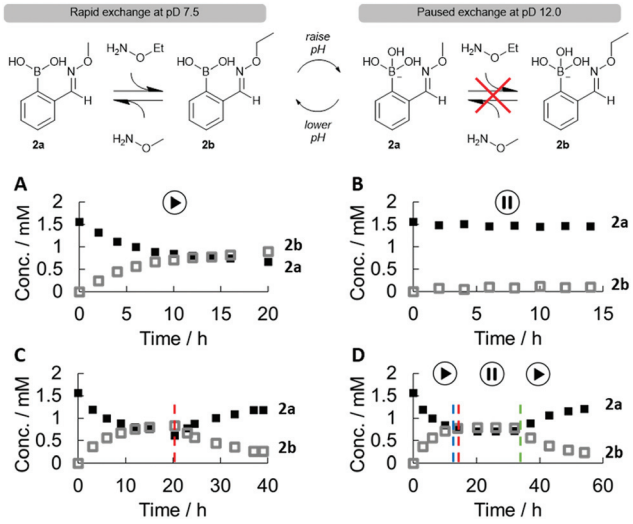

Fig. 6 Pausing and restarting the exchange of 2-FPBA oximes. (A) **2a** was formed *in situ* from 2-FPBA and MHA (3 equiv.) in aqueous buffer (200 mM PB, pD 7.5) and subsequently treated with EHA (3 equiv.) to equilibrate with **2b** at pD 7.5. (B) Under the same conditions as (A) but at pD 12.0, the exchange does not occur. (C) Equilibrating between **2a** and **2b** as in (A) but followed with an additional aliquot of EHA (24 equiv., dashed red line) drives the equilibrium to a **2a**:**2b** ratio of 18:82. (D) Establishing an equilibrium between **2a** and **2b** as in (A) followed by a pD adjustment to 12.0 (dashed blue line) and addition of another aliquot of EHA (24 equiv., dashed red line) does not initiate exchange until the pD is adjusted back to 7.5 (dashed green line).

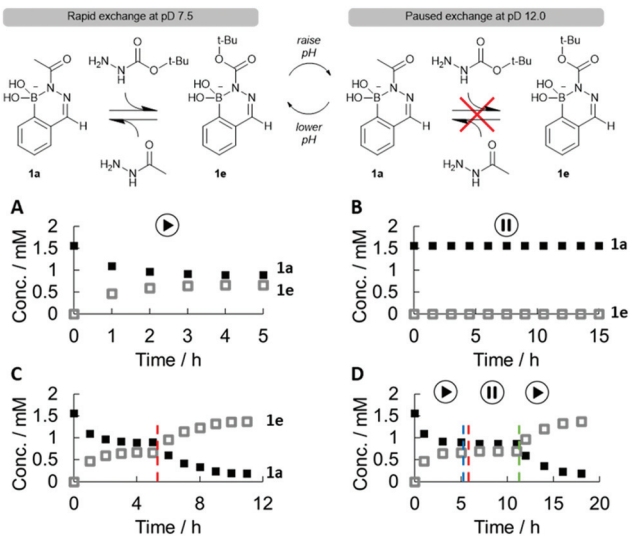

Fig. 5 Pausing and restarting the exchange of 2-FPBA diazaborines. (A) **1a** was formed *in situ* from 2-FPBA and AHz (3 equiv.) in aqueous buffer (200 mM PB, pD 7.5) and subsequently treated with tBCz (0.5 equiv., tBCz) to equilibrate with **1e** at pD 7.5. (B) If the pD is adjusted to 12 before adding tBCz (0.5 equiv.), the exchange does not occur. (C) **1a** and **1e** were initially equilibrated as in (A), and the resulting mixture was treated with an additional aliquot of tBCz (2.5 equiv., dashed red line). The resulting mixture equilibrated to a **1a**:**1e** ratio of 12:88. (D) When the pD was adjusted to 12.0 (dashed blue line) before adding the second aliquot of tBCz (2.5 equiv., dashed red line), no subsequent exchange occurred for 15 hours. Readjusting the pD to 7.5 (dashed green line) immediately resumed the subsequent exchange.

82% **2a**. However, when we adjusted the pD to 12 prior the addition of 24 equivalents of MHA, the mixture showed no subsequent exchange. When the pD was readjusted to 7.5, the exchange immediately resumed; after 20 hours, the mixture equilibrated to 83% oxime **2a** (Fig. 6D). Taken together, these experiments demonstrate that pH control can pause and reactivate exchange dynamics of 2-FPBA-derived DAB and oximes.

Next, we explored strategies to irreversibly abolish the rapid dynamics with an orthogonal input to pH control. Arylboronic acids undergo H_2O_2-mediated oxidation to their corresponding phenols.[35,36] Because the rapid dynamics of 2-FPBA-derived hydrazones and oximes results from activation of the carbonyl by the proximal boronic acid group, we recognized that oxidation would effectively replace the boronic acid with a hydroxyl group. We thus hypothesized that treatment of DAB **1a** and oxime **2a** with H_2O_2 would serve as a mild molecular input to abolish the rapid exchange dynamics.

In support of this hypothesis, we first measured the k_1 and k_{-1} for hydrazone and oxime formation from salicylaldehyde (Sal). The reaction of Sal and AHz yields acyl hydrazone **3** (ESI Fig. S19†), which forms with a rate constant of 2.6×10^{-3} M^{-1} s^{-1} and hydrolyzes with a rate constant of 4.8×10^{-7} s^{-1}. Thus, hydrazone **3**, which is derived from salicylaldehyde, forms 5 orders of magnitude more slowly and hydrolyzes 3-orders of magnitude more slowly than 2-FPBA-derived DAB **1a**. The reaction of Sal and MHA yields oxime **4a** (Fig. 7A). **4a**, derived from salicylaldehyde, forms and hydrolyzes more slowly (k_1 = 1.4 ×

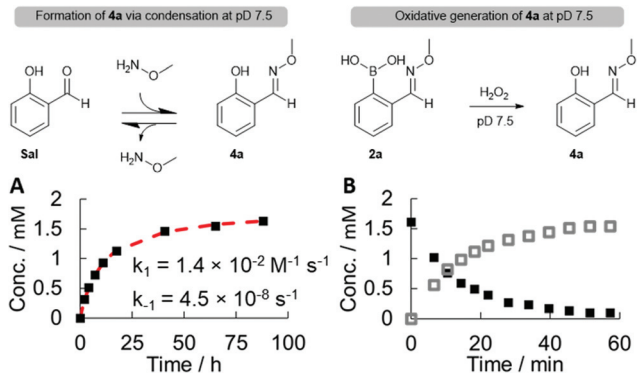

Fig. 7 The dynamics of an oxime with an *ortho* hydroxy is slower than that of an oxime with an *ortho* boronic acid. (A) The reaction of salicylaldehyde (1.85 mM) with MHA (1.85 mM) at pD 7.5 forms **4a** 5-orders of magnitude slower and hydrolyzes 3-orders of magnitude slower than 2-FPBA-derived **2a**. (B) Conversion of the **2a** to **4a** with H_2O_2 (3 equiv.) is complete in about 1 h.

10^{-2} M^{-1} s^{-1}; $k_{-1} = 4.5 \times 10^{-8}$ s^{-1}) than 2-FPBA-derived **2a**. Thus, replacing the boronic acid with a phenol slows the rate of formation by more than 34 000 times and slows the rate of hydrolysis by more than 8000 times. In contrast to oxime **2a**, which has a hydrolytic half-life of *ca.* 50 minutes at 15 °C at physiological pH, the oxidized product has a hydrolytic half-life of almost 6 months. Thus, oxidation of **1a** and **2a** into **3** and **4a**, respectively, should effectively abolish the rapid dynamics of the bond with oxidation.

Oxime **2a** oxidizes cleanly to **4a** with H_2O_2 as revealed by time-course NMR spectroscopy (Fig. 7B and Fig. S20a, S21b†). A near quantitative oxidation was achieved within 1 hour. DAB **1a** also undergoes H_2O_2-mediated conversion to its corresponding phenol **3** (Fig. S22†). In contrast to the oxidation of oxime **2a** to its phenol, which is complete in 1 hour, the oxidation of **1a** takes more than 2 days at room temperature.[37] Reversibility assays reveal that **3** is resistant to exchange. After 15 hours, no observable exchange was observed between **3** and each hydrazide (Fig. S23–S26†) or between **4a** and each alkoxyamine (Fig. 8A and Fig. S27–S29†).

Next, we reasoned that a target oxime population could be established by using the 2-FPBA and then 'cementing' it with oxidation. Oxime **2a** was formed *in situ* with MHA (3 equiv.) and treated with EHA (3 equiv.) at pD 7.5 in buffered D_2O. When the mixture was oxidized with H_2O_2 (3 equiv.) and then treated with 24 equivalents of MHA, no subsequent exchange was observed over the course of 18 hours (Fig. 8B). Thus, in contrast to pH inputs that enable reversible pausing and activation of the exchange dynamics, oxidation irreversibly abolishes the rapid dynamics of 2-FPBA-derived oximes, even at physiological pH.

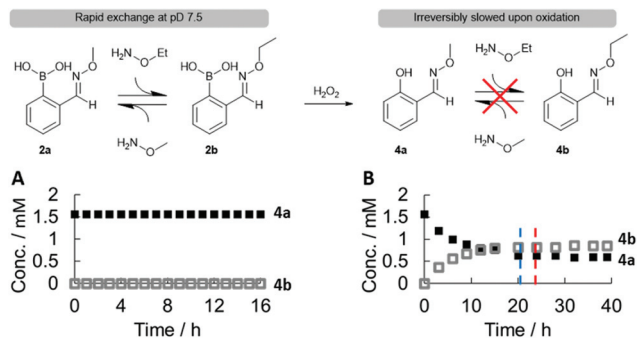

Fig. 8 Unlike oxime **2a**, oxime **4a** does not undergo exchange at pD 7.5 (A) Oxime **4a** does not exchange with EHA (3 equiv.) at pD 7.5. (B) Treating **4a** with EHA (3 equiv.) establishes an equilibrium between **4a** and **4b** after 12 h. After H_2O_2-mediated oxidation (3 equiv., dashed blue line), the addition of additional EHA (24 equiv., dashed red line) does not initiate exchange.

Conclusions

To close, we have presented a kinetic characterization of 2-FPBA-derived hydrazones and oximes that accounts for both their rapid formation and relatively fast hydrolysis. This kinetic analysis reveals that the resulting diazaborines and oximes have K_{eq} values on the order of 10^5–10^6 in the pH range 6.5–12.0. We further demonstrate that small alkyl hydrazides undergo facile exchange with DAB **1a**, even when the competing hydrazide has a strong electron withdrawing group. Sterically congested hydrazides, however, show little to no exchange. Alkoxyamines in exchange with oxime **2a** are comparatively unaffected by steric effects. The rate of exchange can be temporarily paused by raising the pH and restarted by returning to physiological pH. Finally, we demonstrate that the rapid dynamics can be irreversibly abolished by oxidizing the proximal boronic acid to a phenol, which removes the neighboring group catalysis. Taken together, these results enable control over the formation kinetics and exchange dynamics and offer new avenues for reversible bioconjugation and dynamic combinatorial library generation.

Author contributions

G.H. and D.W.D. conceptualized the research. G.H. collected the data. G.H. and D.W.D analyzed the data, and G.H. and D. W.D. wrote the manuscript.

Conflicts of interest

There are no conflicts to declare.

Acknowledgements

This work was supported by start-up funds from the Colorado School of Mines and the Colorado Office of Economic Development and International Trade Advanced Industries Proof-of-Concept grant. We are indebted to Dr Thomas Lee, the director of the Central Analytical Laboratory and Mass

Spectrometry Facility at the University of Colorado, Boulder for helping with the mass analysis of the compounds. The purchase of Waters Synapt G2 HDMS was made possible by National Institute of Health grant S10-RR026641.

Notes and references

1 Y. Jin, C. Yu, R. J. Denman and W. Zhang, *Chem. Soc. Rev.*, 2013, **42**, 6634.
2 Y. Jin, Q. Wang, P. Taynton and W. Zhang, *Acc. Chem. Res.*, 2014, **47**, 1575–1586.
3 S. Ulrich, *Acc. Chem. Res.*, 2019, **52**, 510–519.
4 A. Dirksen, S. Dirksen, T. M. Hackeng and P. E. Dawson, *J. Am. Chem. Soc.*, 2006, **128**, 15602–15603.
5 R. Nguyen and I. Huc, *Chem. Commun.*, 2003, 942.
6 L. Shen, N. Cao, L. Tong, X. Zhang, G. Wu, T. Jiao, Q. Yin, J. Zhu, Y. Pan and H. Li, *Angew. Chem.*, 2018, **130**, 16724–16728.
7 B. Levrand, W. Fieber, J.-M. Lehn and A. Herrmann, *Helv. Chim. Acta*, 2007, **90**, 2281–2314.
8 B. Levrand, Y. Ruff, J.-M. Lehn and A. Herrmann, *Chem. Commun.*, 2006, 2965–2967.
9 K. Kim, H. J. Cho, J. Lee, S. Ha, S. G. Song, S. Kim, W. S. Yun, S. K. Kim, J. Huh and C. Song, *Macromolecules*, 2018, **51**, 8278–8285.
10 M. N. Chaur, D. Collado and J.-M. Lehn, *Chem. – Eur. J.*, 2011, **17**, 248–258.
11 S. R. Beeren, M. Pittelkow and J. K. M. Sanders, *Chem. Commun.*, 2011, **47**, 7359.
12 S. Pfander and R. Fiammengo, *Nucleic Acids Res.*, 2007, **35**, 8.
13 A. Canal-Martín and R. Pérez-Fernández, *ACS Omega*, 2020, **5**, 26307–26315.
14 D. Larsen, A. M. Kietrys, S. A. Clark, H. S. Park, A. Ekebergh and E. T. Kool, *Chem. Sci.*, 2018, **9**, 5252–5259.
15 V. T. Bhat, A. M. Caniard, T. Luksch, R. Brenk, D. J. Campopiano and M. F. Greaney, *Nat. Chem.*, 2010, **2**, 490–497.
16 E. T. Kool, D.-H. Park and P. Crisalli, *J. Am. Chem. Soc.*, 2013, **135**, 17663–17666.
17 O. Dilek, A. Sorrentino and S. Bane, *Synlett*, 2016, **27**, 1335–1338.
18 P. Schmidt, L. Zhou, K. Tishinov, K. Zimmermann and D. Gillingham, *Angew. Chem., Int. Ed.*, 2014, **53**, 10928–10931.
19 P. L. Higgs, A. J. Ruiz-Sanchez, M. Dalmina, B. R. Horrocks, A. G. Leach and D. A. Fulton, *Org. Biomol. Chem.*, 2019, **17**, 3218–3224.
20 P. Schmidt, C. Stress and D. Gillingham, *Chem. Sci.*, 2015, **6**, 3329–3333.
21 O. Dilek, Z. Lei, K. Mukherjee and S. Bane, *Chem. Commun.*, 2015, **51**, 16992–16995.
22 A. Bandyopadhyay and J. Gao, *Chem. – Eur. J.*, 2015, **21**, 14748–14752.
23 M. J. S. Dewar and R. C. Dougherty, *J. Am. Chem. Soc.*, 1964, **86**, 433–436.
24 M. J. S. Dewar and R. C. Dougherty, *J. Am. Chem. Soc.*, 1962, **84**, 2648–2649.
25 P. Tschampel and H. R. Snyder, *J. Org. Chem.*, 1964, **29**, 2168–2172.
26 H. R. Snyder, A. J. Reedy and Wm. J. Lennarz, *J. Am. Chem. Soc.*, 1958, **80**, 835–838.
27 H. Gu, T. I. Chio, Z. Lei, R. J. Staples, J. S. Hirschi and S. Bane, *Org. Biomol. Chem.*, 2017, **15**, 7543–7548.
28 C. J. Stress, P. J. Schmidt and D. G. Gillingham, *Org. Biomol. Chem.*, 2016, **14**, 5529–5533.
29 T. I. Chio, H. Gu, K. Mukherjee, L. N. Tumey and S. L. Bane, *Bioconjugate Chem.*, 2019, **30**, 1554–1564.
30 S. Cambray and J. Gao, *Acc. Chem. Res.*, 2018, **51**, 2198–2206.
31 L. K. Charkoudian, D. M. Pham and K. J. Franz, *J. Am. Chem. Soc.*, 2006, **128**, 12424–12425.
32 L. K. Charkoudian, D. M. Pham, A. M. Kwon, A. D. Vangeloff and K. J. Franz, *Dalton Trans.*, 2007, 5031.
33 L. K. Charkoudian, T. Dentchev, N. Lukinova, N. Wolkow, J. L. Dunaief and K. J. Franz, *J. Inorg. Biochem.*, 2008, **102**, 2130–2135.
34 Q. Wang and K. J. Franz, *Bioorg. Med. Chem. Lett.*, 2017, **27**, 4165–4170.
35 H. G. Kuivila, *J. Am. Chem. Soc.*, 1954, **76**, 870–874.
36 H. G. Kuivila and K. A. Armour, *J. Am. Chem. Soc.*, 1957, **79**, 5659–5662.
37 The origin of the substantial rate difference between the oxidation of a 2-FPBA-derived diazaborines and oximes is currently under investigation in our laboratory and will be reported shortly.